Atmospheric
Chemistry
and Physics
Discussions

Open Access

1   **Influence of enhanced Asian NO$_x$ emissions on ozone in the Upper Troposphere and**

2   **Lower Stratosphere (UTLS) in chemistry climate model simulations**

3   Chaitri Roy[1], Suvarna Fadnavis[1], Rolf Müller[2,] Ayantika Dey Chaudhary[1] and Felix Ploeger[2]

4   [1]Indian Institute of Tropical Meteorology, Pune, India

5   [2]Forschungszentrum Jülich GmbH, IEK7, Jülich, Germany

6   Email of corresponding author: suvarna@tropmet.res.in

7

8   **Abstract:**

9   Asian summer monsoon convection plays an important role in efficient vertical transport from the

10   surface to the anticyclone. In this paper we investigate the potential impact of convectively transported

11   anthropogenic nitrogen oxides (NO$_x$) on the distribution of ozone in the Upper Troposphere and Lower

12   Stratosphere (UTLS) from simulations with the fully-coupled aerosol chemistry climate model,

13   ECHAM5-HAMMOZ. We performed anthropogenic NO$_x$ emission sensitivity experiments over India

14   and China. In these simulations, anthropogenic NO$_x$ emissions for the period 2000-2010 have been

15   increased by 38% over India and by 73% over China in accordance with satellite observed trends over

16   India of 3.8 % per year and China of 7.3% per year. These NO$_x$ emission sensitivity simulations show

17   that strong convection over the Bay of Bengal and the Southern slopes of the Himalayas transports

18   Indian emissions into the UTLS. Convective transport from the South China Sea injects Chinese

19   emissions into the lower stratosphere. Indian and Chinese emissions are partially transported over the

20   Arabian Sea and west Asia by the tropical easterly jet. Enhanced NO$_x$ emissions over India and China

21   increase the ozone radiative forcing over India by 0.112 W/m^2 and 0.121 W/m^2 respectively. These

22   elevated emissions produces significant warming over the Tibetan Plateau and increase precipitation

23   over India due to a strengthening of the monsoon Hadley circulation.

24   However doubling of NO$_x$ emissions over India (73%); equal to China, produced high ozone in the

Atmospheric
Chemistry
and Physics
Discussions

25 lower troposphere. It induced a reverse monsoon Hadley circulation and negative precipitation

26 anomalies over India. The associated subsidence suppressed vertical transport of NO_x and ozone into

27 the anticyclone.

28 Key words: Asian summer monsoon, Ozone, increase in tropospheric NO_x, NO_x transport, Upper

29 troposphere and lower stratosphere.

30

31 **1. Introduction**

32   Rapid economic development and urbanization in Asia has resulted in an unprecedented growth

33 in anthropogenic emissions like nitrogen oxides (NO_x), carbon monoxide (CO), carbon dioxide (CO_2),

34 methane (CH_4,), etc. Many of these species have implications on tropospheric ozone (Wild and

35 Akimoto, 2001; IPCC, 2001). Ground based and satellite observations show a high amount of these

36 ozone precursors concentrated over the India and China (Sinha et al., 2014; Richter et al., 2005; Jacob

37 et al., 1999; Zhao et al., 2013; Gu et al., 2014). Recent studies show that tropospheric ozone production

38 over Asia is controlled by the abundance of NO_x and VOCs and the ratios of these species (Sillman,

39 1995, Lei et al., 2004, Zhang et al., 2004 and Tie et al., 2007). These studies reveal that in Asia,

40 particularly India and China are NO_x limited regions, i.e., controlling NOx in these regions would

41 reduce ozone concentrations (Yamaji et al., 2006; Sinha et al., 2014; Fadnavis et al., 2014). Thus levels

42 of tropospheric ozone, a key polluting agent and greenhouse gas, are controlled by NO_x concentration

43 over these regions. Recently, a positive trend of 3.8 % yr^{-1} (for the period 2003-2011) in tropospheric

44 column NO_2 over India has been reported using SCanning Imaging Absorption SpectroMeter for

45 AtmosphericCHartographY (SCIAMACHY) observations (Ghude et al., 2013) and of 7.3% yr^{-1} (for the

46 period 2002-2011) over China from Ozone Monitoring Instrument (OMI) observations (Schneider and

47 van der A, 2012). Apart from anthropogenic sources, lightning also contributes to the production of

48 NOx. Over the Asian region, in the middle and upper troposphere, lightning contributes ~40% to NO_x

49   and 20% to ozone production during monsoon season (Tie et al 2001; Fadnavis et al 2015). The upper

50   tropospheric ozone concentration is determined both by in-situ production as well as from convective

51   transport from the boundary layer (Søvde et al., 2011).

52   Ozone in the troposphere absorbs relatively little UV radiation but it has a huge climatic impact

53   (Lacis et al., 1990). The estimated global average radiative forcing increasing tropospheric ozone since

54   pre-industrial times is estimated to be $+0.35 \pm 0.15$ Wm^{-2} (IPCC, Ramaswamy et al., 2001). Previous

55   studies revealed that ozone perturbations exert a large influence on temperature near the surface and

56   tropopause (e.g., Thuburn and Craig, 2002; Foster and Shine 1997). Thus the tropospheric ozone

57   distribution and its variability at different altitudes influence the thermal structure of the atmosphere.

58   Climate change due to ozone variations is highest near the tropopause because the greenhouse

59   efficiency per molecule is highest there (Lacis et al, 1990; Forster and Shine, 1997; Riese et al., 2012).

60   A study based on ACCMIP models reports that NO_X and CH_4 are the greatest contributors in

61   determining ozone radiative forcing (Stevenson et al., 2013).

62   Asian Summer Monsoon (ASM) convection efficiently transports Asian pollutants from the

63   boundary layer into the Upper Troposphere and Lower Stratosphere (UTLS) (Randel and Park, 2006;

64   Randel et al. 2010; Fadnavis et al., 2013, 2015). Studies pertaining to modeling and trajectory analysis

65   confirm this finding (Li et al., 2005; Park et al., 2007; Randel et al., 2010; Chen et al., 2012; Vogel et

66   al., 2015). Satellite observations show the confinement of a number of chemical constituents like water

67   vapor (H_2O), CO, ethane (C_2H_6), CH_4, nitrous oxide (N_2O), hydrogen cyanide (HCN), and aerosols,

68   within the ASM anticyclone (Randel et al. 2010; Li et al., 2005; Randel and Park, 2006; Lawrence et

69   al., 2011) which has potential implication on stratospheric chemistry and dynamics. These studies

70   indicate that the rise in anthropogenic emissions over the ASM region alters the chemical composition

71   of the UTLS (Lawrence et al., 2011; Fadnavis et al, 2014, 2015) during the monsoon season. Another

72   prominent feature of the satellite observations is an ozone minimum in the ASM anticyclone (near 100

73   hPa) (Gettelman et al., 2004; Konopka et al., 2010; Braesicke et al., 2011). This ozone minimum is

74   linked to ozone poor air masses arriving from the Bay of Bengal and Arabian Sea. Balloonsonde

75   observations show that ozone variations near the anticyclone are strongly correlated with temperature

76   near the tropopause (Tobo et al., 2008). Thus observations show that convectively lifted air masses

77   arriving in the anticyclone are ozone poor but rich in ozone precursors. Thus the linkage of low ozone

78   and high ozone precursors with temperature variation in the anticyclone is an open question. In this

79   study we ask the question 'how do rising Asian NO_X (an important ozone precursor) emissions and

80   associated ozone production affect the ozone radiative forcing and monsoon circulation?' For this we

81   perform anthropogenic NO_x emission sensitivity experiments using the state-of-the-art ECHAM5-

82   HAMMOZ (European Centre General Circulation Model version5) chemistry climate model (Roeckner

83   et al., 2003; Horowitz et al., 2003; Stier et al., 2005). From these simulations ozone radiative forcing

84   for different anthropogenic NO_x emission scenarios is estimated. Associated temperature and monsoon

85   circulation changes are also reported. The paper is organized as follows: data description and model

86   setup are discussed in section 2; results are discussed in section 3. Section 4 comprises of discussion

87   followed by conclusion in section 5.

88

89   **2. Data description and Model setup**

90   **2.1 Satellite measurement**

91   Earth Observing System (EOS) microwave limb sounder (MLS) is a NASA Aura satellite which

92   flies in the polar sun-synchronous orbit. It measures the thermal emissions at millimeter and sub-

93   millimeter wavelengths (Waters et al., 2006). It performs 240 limb scans per orbit with a footprint of

94   ∼6 km across-track and ∼200 km along-track, providing ∼3500 profiles per day. MLS also measures

95   the vertical profiles of temperature, ozone, CO, H_2O, and many other constituents in the mesosphere,

96   stratosphere and upper troposphere (Waters et al., 2006). In the UTLS, MLS has a vertical resolution of

Atmospheric
Chemistry
and Physics
Discussions

97   3 km. MLS vertical profiles of ozone show good agreement with the Stratospheric Aerosol and Gas

98   Experiment II (SAGE-II), Halogen Occultation Experiment (HALOE), Atmospheric Chemistry

99   Experiment (ACE) and ozonesonde measurements (Froidevaux et al.,2006). The MLS ozone profiles

100   are considered to be useful in the range of 215 − 0.46 hPa (Livesey et al., 2005). In this study we

101   analyze the MLS level 2 (version 4) ozone mixing ratios data for the period 2004 − 2013. The data has

102   been gridded at 8.3º×3º. This data can be accessed from http://mls.jpl.nasa.gov/. For comparison

103   simulated ozone is convolved with the MLS averaging kernel. Details of MLS averaging kernels are

104   documented by Livesey et al. (2011).

105

106   **2.2 Model simulation and experimental setup**

107   We employ the aerosol-chemistry-climate model ECHAM5-HAMMOZ which comprises the

108   general circulation model ECHAM5 (Roeckner et al., 2003), the tropospheric chemistry module, MOZ

109   (Horowitz et al 2003) and the aerosol module, Hamburg aerosol model (HAM) (Stier et al., 2005). It

110   includes NO_x, VOC and aerosol chemistry. The gas phase chemistry is based on the chemical scheme

111   provided by the MOZART-2 model (Horowitz et al., 2003) which includes detailed chemistry of the

112   O_X-NO_X hydrocarbon system with 63 tracers and 168 reactions. The $O(^1D)$ quenching reaction rates

113   were updated according to Sander et al., (2003) and isoprene nitrates chemistry according to Fiore et

114   al., (2005). The dry deposition in ECHAM5-HAMMOZ follows the scheme given by Ganzeveld and

115   Lelieveld (1995). Soluble trace gases like HNO_3 and SO_2 are also subject to wet deposition. In-cloud

116   and below-cloud scavenging follows the scheme given by Stier et al. (2005).

117   The model is run at a T42 spectral resolution corresponding to about 2.8°×2.8° in the horizontal

118   dimension and 31 vertical hybrid σ − p levels from the surface to 10 hPa. The details of model

119   parameterizations, emissions and validation are described by Fadnavis et al. (2013; 2014; 2015) and

120   Pozzoli et al. (2008a, b; 2011). The base year for trace gas emissions is taken as 2000. Each member of

Atmospheric
Chemistry
and Physics
Discussions

121   our sensitivity study consists of continuous simulations for eleven years from 2000 to 2010. For each

122   simulation emissions were the same. Meteorology varied due to varying sea surface temperature (SST)

123   and sea ice (SIC). The AMIP2 SSTs and SIC representative of the period $2000 - 2010$ were specified as

124   a lower boundary condition.

125   In order to understand the impact of increasing NO_x emissions on the distribution of ozone in

126   the UTLS, simulations were performed for the period $2000 - 2010$. The experimental set up is the same

127   as described by Fadnavis et al., (2015). The four experiments analyzed in this study are (1) A reference

128   experiment (CTRL) and three sensitivity experiments (referred to as experiments 2 - 4), where the NO_X

129   emissions over India and China are scaled in accordance with the observed trends. In experiment (2),

130   NO_X emissions are increased over India by 38% (Ind38), in experiment (3) increases that over China

131   by 73% (Chin73) are prescribed. In order to analyze the effects of equal NO_x emissions over India and

132   China, NO_x emissions are increased over India by 73% over India (Ind73) in experiment (4). The

133   emission perturbations were obtained from observed NO_2 trends of 3.8% per year over India (Ghude et

134   al., 2013) and 7.3% per year over China (Schneider and van der A, 2012). Hiboll et al., (2013) also

135   reported similar increasing NO_x values over megacities in India and China.

136   To calculate the heating associated with ozone changes over India and China, we use the

137   radiative transfer model Santa Barbara DISORT Atmospheric Radiative Transfer (SBDART). This

138   model is designed and developed by the University of California, Santa Barbara (Ricchiazzi et al.,

139   1998) and is based on a collection of well-tested and reliable physical models. We used eight streams in

140   the radiative transfer calculation and computations were made for solar zenith angles at every 5°.

141

142   **3. Results**

143   **3.1 Comparison with AIRS satellite measurements in the UTLS**

144   Figure 1(a) shows the spatial distribution of MLS ozone mixing ratios at 100 hPa. The

Atmospheric
Chemistry
and Physics
Discussions

145   distribution of simulated ozone mixing ratios at the nearest model level, 90 hPa is plotted in figure 1(b).

146   ECHAM5-HAMMOZ simulation is smoothed with averaging kernel of MLS. The winds plotted in

147   figure 1(a) and 1 (b) show the extent of the monsoon anticyclone ($20^{°}$E-$120^{°}$E). Winds plotted in figure

148   1(b) depict the extent of the monsoon anticyclone ($20^{°}$E-$120^{°}$E). The spatial pattern of low ozone

149   concentrations in the monsoon anticyclone is well simulated in the model. In the recent past, low

150   ozone mixing ratios (~40-160 ppbv) in the monsoon anticyclone have been reported from MLS (90-140

151   ppbv), MIPAS (80-120 ppbv), SAGE II (<150ppbv) measurements (Kunze et al., 2010; Randel et al.,

152   2001; Randel and Park 2006; Park et al., 2007). Vertical profiles of ozonesonde (averaged for the

153   monsoon season during 2001-2009) at Indian stations, Delhi (28.61ºN, 77.23ºE), Pune (18.52ºN,

154   73.85ºE) and Thiruvananthapuram (8.48ºN, 76.95E) are compared with MLS measurements and

155   ECHAM5-HAMMOZ simulated ozone mixing ratios in figures 1(c)-(e). These figures depict that

156   vertical variation of simulated ozone show good agreement with ozonesonde and MLS observations.

157   Fadnavis et al., (2015) compared the model simulation with aircraft observations over the various

158   regions all over the globe during the monsoon season. This study reported a reasonable agreement for

159   PAN, NOx, HNO$_3$ and ozone mixing ratio.

160

161   **3.2 Transport of enhanced NO$_x$ emissions into the UTLS**

162   Recent satellite observations and model simulations established the impact of convective

163   transport of boundary layer pollution into the ASM anticyclone during the Asian monsoon season

164   (Gettelman et al., 2004; Randel et al., 2010; Fadnavis et al., 2013, 2014, 2015). These pollutants are

165   further transported across the tropopause as evident in satellite observations of, e.g. water vapour (Bian,

166   2012), hydrogen cyanide (HCN) (Randel, 2010), CO (Schoeberl et al., 2006), Peroxyacetyl nitrate

167   (PAN), aerosols (Vernier et al., 2015, Fadnavis et al 2013) etc. To understand the influence of monsoon

168   convection on the vertical distribution of NO$_x$ we show zonal and meridional cross sections over India

Atmospheric
Chemistry
and Physics
Discussions

169   and China. The vertical distribution of NO_x averaged for the monsoon season over the Indian latitudes

170   (8°-35°N), and Chinese latitudes (20°-40°N) as obtained from CTRL simulations is shown in the

171   supplementary figures S1(a) and S1(b) respectively. These figures show elevated levels of NO_x

172   extending from the surface to the upper troposphere (UT) over India and China. The wind vectors

173   along with the distribution of cloud droplet number concentration and ice crystal number concentration

174   together, (Figure S2(a) and S2(b)) indicate strong convective transport from the Bay of Bengal (BOB),

175   southern slopes of Himalayas, and south China Sea which might lift the boundary layer NO_x to the

176   upper troposphere.

177   During the monsoon season, the NO_x distribution in the UTLS is influenced by lightning apart

178   from transport from anthropogenic sources. In this season, lightning activity is highest in Asia

179   (Ranalkar and Chaudhari, 2009; Penki and Kamra, 2013) compared to the other monsoon regions

180   (North America, South America and Africa). However, in our simulations there is no contribution from

181   lightning.

182   We show longitude-pressure (Figures 2(a)-(c)) and latitude-pressure sections (Figures 2(d)-(f))

183   of anomalies of anthropogenic NO_x obtained from Ind38, Ind73, Chin73 with respect to CTRL

184   simulations. The black arrows indicate the anomalies of wind vectors. Ind38 and Chin73 simulations

185   (Figures 2(a) and 2(d)) show that the convective winds at the southern flank of the Himalayas (80°-

186   90°E) and over the Bay of Bengal lift up the enhanced NO_x emissions to the upper troposphere (UT).

187   The majority of the outflow is into the UT and only part of it is transported into the lower stratosphere.

188   Cross tropopause transport due to convection over South China Sea is evident in the Chin73 simulation

189   (Figure 2(c) and 2(f)). Previous studies also indicate significant vertical transport due to strong

190   monsoon convection from the southern slopes of Himalayas (Fu et al., 2006, Fadnavis et al., 2013;

191   2014) and the South China sea (Park et al 2009; Chen et al., 2012), which is in agreement with our

192   results. In the upper troposphere, NO_x is transported over Iran and Saudi Arabia along the descending

193   branch of circulation.

194   However the simulation with doubled NO_x emissions over India (Ind73) does not show cross

195   tropopause transport. The wind anomalies show a descending branch over central India (~20°N, 75°E)

196   (Figures 2(b) and 2(e)) which might have inhibited the cross-tropopause transport in the Ind73

197   simulation. The descending wind anomalies may be related to ozone radiative forcing and associated

198   temperature changes (discussed later in section 4).

199   Figures 2(d) and 2(f) also indicate transport of NO_x from India and China across the tropopause

200   and entrainment into the tropical pipe. Garny and Randel (2013) and Randel et al. (2010) also reported

201   that pollution transported by Asian monsoon convection enters the deep stratosphere via the tropical

202   pipe.

203

204   **3.3 Impact of enhanced anthropogenic NO_x on the tropospheric ozone distribution**

205   Tropospheric ozone is a radiatively active trace gas (Ramanathan et al., 1987) therefore it is

206   important to know the impact of enhanced NO_x emissions on tropospheric ozone production (Derwent,

207   1990). We estimate the change in ozone production due to enhanced NO_x emissions in the Ind38, Ind73

208   and Chin73 simulations with respect to CTRL. The longitude-pressure cross sections of changes in

209   amount of net ozone production (%) over India and China are shown in figures 3(a)-(c). It can be seen

210   that at the altitudes below 300 hPa there is ozone production and loss varying in between -60% to

211   +60%. In the upper troposphere (300-150hPa), the estimated amount of net ozone production in Ind38

212   and Ind73 simulation is ~5-10% and that from Chin73 simulation is ~10-30%. Comparison of figures 2

213   and 3 show that ozone production by NO_x photolysis occur in the regions where there is a transport of

214   NO_x. In Ind73 simulation there is no change in ozone production near the tropopause as the NO_x

215   emissions do not reach up to these altitudes (Figures 2(b) and 2(e)). In the Ind73 simulation there is

216   significant increase in net ozone production (~40-90% between 1000-500 hPa) over the Indo Gangetic

Atmospheric
Chemistry
and Physics
Discussions

Open Access

EGU

217   Plain (figure not included).

218   Figures 4(a)-(c) show the longitude-pressure distribution of ozone mixing ratio anomalies

219   obtained from Ind38 and Ind73 averaged over 8°-35°N, and Chin73 over 20°-45°N. Although the air

220   mass in the monsoon anticyclone is poor in ozone (Figure 1(b)), the elevated ozone anomalies in

221   response to increased NO_x emissions are seen in figure 4 (in the Ind38 and Chin73 simulations). This

222   may be partially due to transported ozone via ASM convection and partially due to production of ozone

223   (Figures 3 and 4); there is no contribution from lightning in our simulations. It can be seen from figures

224   4(a)-(c) that ozone levels are enhanced near 300-200 hPa over Arabia. This may be due to the ASM

225   vertical convective transport and subsequent horizontal transport in the monsoon anticyclone (Randel et

226   al., 2010, Garny and Randel, 2013; Vogel et al., 2015).

227   Latitude-pressure cross section of ozone anomalies plotted in figures 4(d) and 4(f) show that

228   convection over the Bay of Bengal, southern slopes of the Himalayas and the South China Sea lifts

229   ozone from India and China into the upper troposphere and it is then transported across the tropopause

230   into the tropical pipe. Ozone and NO_x transported across the tropopause will enhance their amount in

231   the surf mixing zone above the tropopause (Vogel et al., 2015). In the lower stratosphere there will be

232   ozone production by photolysis from transported NO_x.

233   Doubling of NO_x emissions over India (Ind73) results in a descending branch of circulation

234   over central India (Figures 4(b) and 4(e)). This subsidence suppressed the vertical transport of ozone

235   across the tropopause. It is also evident in NO_x distribution (Figures 2(b) and 2(e)). As discussed

236   earlier, this subsidence may be related to temperature changes due to ozone radiative forcing and

237   heating rates as there is significant increase in ozone production over the Indo Gangetic plain (1000 –

238   500 hPa) (discussed in section 4).

239

240   **3.4 Ozone distribution in the anticyclone**

Atmospheric
Chemistry
and Physics
Discussions

Open Access

EGU

241   We estimate changes in NO_x and ozone in the monsoon anticyclone from Ind38, Ind73 and

242   Chin73 simulations with respect to the CTRL simulation. The distribution of these species is shown at

243   110 hPa as representative for the anticyclone. Figures 5(a)-(c) depict percentage changes in NO_x

244   mixing ratios for Ind38, Ind73 and Chin73 simulations. A maximum in the NO_x anomalies in the ASM

245   anticyclone (20°E to 120°E) is seen in all the simulations. Ozone anomalies are high at the eastern part

246   of monsoon anticyclone since convective injection into the anticyclone occurs at the eastern part of

247   anticyclone (Fadnavis et al., 2013). Percentage increase in NO_x amounts in the Ind38 simulation is

248   higher (Figure 5(a)) than that in the Ind73 simulation (Figure 5(b)). This is mainly due to descending

249   motion over the central India, as seen in the previous sections. However, the Chin73 simulation shows

250   higher values of increasing NO_x (>18%) in the monsoon anticyclone (Figure 5(c)). In the anticyclone,

251   the increase in ozone mixing ratios in Ind38 simulation is 1-3%, Ind73 is 1-5% and Chin73 is 1-8%.

252   These figures show that easterly jet transport NOx and ozone (from India and China) to Saudi Arabia,

253   Iran and Iraq.

254

255   **4. Discussion**

256   Increase in ozone mixing ratios may enhance ozone radiative forcing and exert warming

257   (Brasseur, 1997). We estimate anomalies in ozone radiative forcing at the top of the atmosphere for

258   Ind38, Chin73, Ind73 with respect to CTRL simulation over central India (20º-30ºN, 75º-85ºE) and

259   China (30º-45ºN, 100º-135ºE). The increase in ozone radiative forcing over India, in the Ind38

260   simulation is 0.112 W/m^2, and in the Chin73 simulation is 0.121 W/m^2. In comparison, the estimated

261   global average radiative forcing due to increases in tropospheric ozone since pre-industrial times is

262   estimated to be $+0.35 \pm 0.15$ Wm^{-2} (Brasseur et al., 1997; IPCC, Ramaswamy et al., 2001).

263   Further, we analyze the temperature anomalies for the Ind38, Ind73 and Chin73 simulations.

264   Figures 6(a)-(c) show the zonal distribution of temperature anomalies. These simulations show surface

11

Atmospheric
Chemistry
and Physics
Discussions

265   warming over the 30º-40ºN, regions covering North India and North China. The striking feature evident

266   in Ind38, and Chin73 simulations is anomalous warming over the Tibetan Plateau while it is subdued in

267   Ind73 simulation.

268   In order to understand the atmospheric heating caused due to ozone, we calculate the ozone

269   heating rate using the radiative transfer model, SBDART. ECHAM5-HAMMOZ model simulated

270   temperature, pressure, as well as water vapour concentration and ozone concentrations at various levels

271   are incorporated into the SBDART model in order to estimate the ozone heating rate in the vertical.

272   Figure 7(a) shows the vertical profile of ozone radiative heating rate as obtained from CTRL simulation

273   averaged over Indian (70º-94ºE, 20º-30ºN) and Chinese (70º-100ºE, 30º-40ºN) regions. It shows a high

274   value of ~ 0.003- 0.009 K/day at ~1-4 km. A net radiative heating rate of 0.004 – 0.008 K/day in the

275   troposphere due to changes in ozone was earlier reported by Ramaswamy and Bowen (1994).

276   Anomalous warming over the Tibetan plateau seen in Figure 6 may be due to heating caused by

277   ozone. Figure 7(b) shows the vertical distribution of anomalies in ozone heating rates averaged over

278   Tibetan plateau (70-100°E, 20-40°N). Positive ozone heating rate anomaly (0.0005-0.0001 K/day) is

279   seen below14 km in Ind38 and Chin73, on the contrary, Ind73 shows negative anomalies in ozone

280   heating rate below 8 km. In the upper troposphere (8 – 14 km) ozone heating rates are positive in all the

281   simulations. They are less in Ind73 ($2.09 \times 10^{-6} – 4.5 \times 10^{-6}$ K/day) as compared to Ind38 ($1.91 \times 10^{-5} –$

282   2.74×10^{-5} K/day) and Chin73 (2.17×10^{-5} - 2.99×10^{-5} K/day). The estimated heating rates over the

283   Indo Gangetic plain are ~ 3×10^{-4} K/day (averaged over 1000-800 hPa) this may be due to high amount

284   of ozone production. Ozone heating rate anomaly of $\pm 2 \times 10^{-4}$ K/day was previously reported by Guo

285   et al., 2008, over East Asia and the Tibetan plateau region.

286   From figures 3, 6 and 7 it can be said that doubling of NO_x emissions (Ind73 simulation) over

287   India increases net ozone production over Indo Gangetic plain. Enhanced ozone production leads to

288   anomalous ozone heating in the lower troposphere over the Indo Gangetic plain (~3×10^{-4} K/day). This

Atmospheric
Chemistry
and Physics
Discussions

289   elicited reversal of monsoon Hadley cell circulation. The descending branch of monsoon Hadley cell

290   circulation over central India (figures 2 and 4) resisted vertical transport of ozone which resulted in

291   subdued Tibetan plateau warming.

292   The meridional temperature gradient in the upper troposphere over the Tibetan plateau during

293   the monsoon is one of the key factors responsible for the ASM circulation (Flohn 1957; Yanai et al.,

294   1992; Meehl, 1994; Li and Yanai, 1996; Wu and Zhang, 1998). Flohn (1957, 1960) suggested that

295   warming over the Tibetan plateau leads to a reversal of the meridional temperature gradient triggering

296   large-scale change in the general circulation over Asia. The warm ascending air above the Tibetan

297   plateau gradually spreads southward and descends over the northern Indian Ocean. The south-westerly

298   winds at the surface on the other hand complete the Hadley cell. This local circulation system releases

299   latent heat and further maintains the Tibetan high warm core. Thus heating over the Tibetan plateau

300   leads to increased Indian summer monsoon rainfall by enhancing the cross-equatorial circulation and

301   concurrently strengthening both the Somali Jet and the westerly winds that bring rainfall to India

302   (Rajagopalan and Molnar, 2013, Vinoj et al., 2014). Goswami et al., (1999) also reported that there is a

303   strong correlation between Hadley circulation and monsoon precipitation.

304   Figures 8(a)-(c) depict the monsoon Hadley cell circulation (averaged over 70ºE-110ºE)

305   obtained from the Ind38 Ind73 and Chin73 simulations. The Ind38 and Chin 73 simulations show

306   strengthening of the Hadley circulation; a strong ascending branch of the Hadley cell around 20ºN

307   (Figure 8(a)), whereas it is reversed in Ind73 simulation (Figure 8(b)). Consequently, precipitation

308   anomalies over the Indian region are positive (0.3 − 0.9 mm/day) in Ind38 and Chin73 simulations

309   (figure 8(d)) whereas they are negative in Ind73 simulation (-0.3 − -0.6 mm/day) (Figure 9(e)). Thus

310   enhanced Indian and Chinese NO_x emissions increases warming over the Tibetan plateau by ozone

311   heating and enhances precipitation over India via strengthening Hadley circulation. Whereas doubling

Atmospheric
Chemistry
and Physics
Discussions

Open Access

EGU

312   of NO_x emissions over India produced high amount of ozone over the Indo Gangetic plain. Related

313   ozone heating in the lower troposphere reverses the monsoon Hadley circulation and thereby resulted in

314   negative precipitation anomalies.

315

316   **5. Conclusions**

317   In this paper we investigate the potential impacts of enhanced anthropogenic NO_x emissions on

318   ozone production and distribution during the monsoon season using the state-of-the-art ECHAM5-

319   HAMMOZ model simulations. We performed sensitivity experiments for anthropogenic NO_x

320   enhancement, 38% over India (Ind38 simulation) and 73% over China (Chin73 simulation) in

321   accordance with observed trends 3.8% per year over India and 7.3% per year over China (Ghude et al.,

322   2013; Schneider and van der A, 2012). In another experiment, anthropogenic NO_x emissions over India

323   are doubled (73%), equal to China (Ind73 simulation).

324   These simulations show that increase in anthropogenic NO_x emissions (over India and China)

325   increases ozone production in the lower and mid-troposphere. The monsoon convection at the southern

326   flank of the Himalayas (80-90°E) and over the Bay of Bengal lifts up the NO_x and ozone from India

327   across tropopause into the lower stratosphere. Cross tropopause transport also occurs over China due to

328   convection over the South China Sea. These air masses are then transported deeper into the stratosphere

329   via the tropical pipe.

330   Increase in NO_x emissions in Ind38 and Chin73 simulations increases ozone radiative forcing

331   over India by 0.112 W/m^2 and 0.121 W/m^2 respectively. Enhanced ozone production (Ind38 and

332   Chin73 simulations) increases ozone heating rates which cause anomalous warming over the Tibetan

333   plateau. Doubling of NO_x emissions over the India region (Ind73 simulation) produces anomalous

334   heating near surface over the Indo Gangetic plain ($\sim 3 \times 10^{-4}$ K/day) due to high amount of ozone

335   production (~40-90%). This elicited subsidence over central India (via reversal of monsoon Hadley

336   circulation) and resisted vertical transport of ozone which resulted in subdued Tibetan plateau warming.

337   In Ind38 and Chin73 simulations, anomalous warming over the Tibetan plateau resulted in

338   strengthening of the monsoon Hadley circulation over India and elicited positive precipitation (0.3 –

339   0.9 mm/day) anomalies over India. However, doubling of NO_x emissions over India (Ind73) induced

340   reverse Hadley circulation due to anomalous heating, in the lower troposphere over the Indo Gangetic

341   plain. The descending branch of the Hadley circulation resisted the cross tropopause transport of ozone

342   and NO_x. The reversal of the Hadley circulation and concurrent subdued warming over the Tibetan

343   plateau resulted in negative precipitation anomalies (-0.3 – -0.6 mm/day) over India.

344

Atmospheric
Chemistry
and Physics
Discussions

Open Access

EGU

References:

Bian, J., Pan, L. L., Paulik, L., Vömel, H., Chen, H., and Lu, D.: In situ water vapor and ozone measure-ments in Lhasa and Kunming during the Asian summer monsoon, Geophys. Res. Lett., 39, L19808, doi:10.1029/2012GL052996, 2012.

Braesicke, P., Smith, O. J., Telford, P., & Pyle, J. A.: Ozone concentration changes in the Asian summer monsoon anticyclone and lower stratospheric water vapour: An idealised model study. Geophysical Research Letters, 38(3), doi: 10.1029/2010GL046228, 2011.

Brasseur, G.P., Kiehl, J.T., Müller, J.F., Schneider, T., Granier, C., Tie, X. and Hauglustaine, D.: Past and future changes in global tropospheric ozone: Impact on radiative forcing. Geophys. Res. Lett., 25(20), 3807-3810, doi: 10.1029/1998GL900013,1998.

Brasseur, Guy P., Edited. The stratosphere and its role in the Climate System. Vol. 54. Springer Science & Business Media, 2013.

Chen, B., Xu, X., D, Yang, S., and Zhao, T. L.: Climatological perspectives of air transport from atmospheric boundary layer to tropopause layer over Asian monsoon regions during boreal summer inferred from Lagrangian approach, Atmos. Chem. Phys., 12, 5827–5839, doi:10.5194/acp-12-5827-2012. 2012.

Derwent, R. G: Trace Gases and their Relative Contribution to the Greenhouse Effect, AERE Report R-13716, H.M. Stationery Office, London. 1990.

Dunkerton, T. J.: Evidence of meridional motion in the summer lower stratosphere adjacent to monsoon regions, J. Geophys. Res., 100, 16,675–16,688, doi: 10.1029/95JD01263, 1995.

Elampari, K., Chithambarathanu, T., Krishna Sharma, R., and Johnson Jeyakumar, S.: Surface ozone air pollution in Nagercoil, India, Indian Journal of Science and Technology, 4(3), 181-184, doi: 10.17485/ijst/2011/v4i3/29961, 2011.

Fadnavis, S., Semeniuk, K., Pozzoli, L., Schultz, M. G., Ghude, S. D., Das, S., and Kakatkar, R.: Transport of aerosols into the UTLS and their impact on the Asian monsoon region as seen in a global model simulation, Atmos. Chem. Phys., 13, 8771–8786, doi:10.5194/acp-13-8771-2013, 2013.

Fadnavis, S., Semeniuk, K., Schultz, M. G., Mahajan, A., Pozzoli, L., Sonbawane, S., and Kiefer, M.: Transport pathways of peroxyacetyl nitrate in the upper troposphere and lower stratosphere from different monsoon systems during the summer monsoon season, Atmos. Chem. Phys. Discuss., 14, 20159–20195, doi:10.5194/acpd-14-20159-2014, 2014.

Fadnavis, S., Semeniuk, K., Schultz, M. G., Kiefer, M., Mahajan, A., Pozzoli, L., and Sonbawane, S.: Transport pathways of peroxyacetyl nitrate in the upper troposphere and lower stratosphere from different monsoon systems during the summer monsoon season. Atmos. Chem. and Phys., 15, doi:10.5194/acp-15-11477-2015, 11477-11499, 2015.

Fiore, A. M., Horowitz, L. W., Purves, D. W., Levy II, H., Evans, M. J., Wang, Y., Li, Q., and Yantosca, R. M.: Evaluating the contribution of changes in isoprene emissions to surface ozone trends over the eastern United States, J. Geophys. Res., 110, D12303, doi:10.1029/2004JD005485, 2005.

Flohn, H.: Large-scale aspects of the summer monsoon in South and East Asia, J. Meteor. Soc. Japan, 75, 180–186, doi: 551.553.21:551.589.5, 1957.

Flohn, H.: Recent investigations on the mechanism of the "Summer Monsoon" of Southern and Eastern Asia, Proc. Symp. Monsoon of the World, 1960.

Forster, F., Piers, M., and Keith, P. Shine: Radiative forcing and temperature trends from stratospheric ozone changes, J. Geophys Res, 102, 10841-10855, 1997.

Froidevaux, L., Livesey, N. J., Read, W. G., Jiang, Y. B., Jimenez, C. J., Filipiak, M. J., Schwartz, M. J., Santee, M. L., Pumphrey, H. C., Jiang, J. H., Wu, D. L., Manney, G. L., Drouin, B. J.,

Atmospheric
Chemistry
and Physics
Discussions

393   Waters, J. W., Fetzer, E. J., Bernath, P. F., Boone, C. D., Walker, K. A., Jucks, K. W., Toon, G.
394   C., Margitan, J. J., Sen, B., Webster, C. R., Christensen, L. E., Elkins, J. W., Atlas, E., Ueb, R.
395   A., and Hendershot, R.: Early validation analyses of atmospheric profiles from EOS MLS on
396   the Aura satellite. IEEE Trans. Geosci. Remote Sensing 44, 1106 – 1121, doi:
397   10.1109/TGRS.2006.864366, 2006.
398   Fu, R., Hu, Y. L., Wright, J. S., Jiang, J. H., Dickinson, R.E., Chen, M. X., Filipiak, M., Read, W. G.,
399   Waters, J. W.,and Wu, D. L.: Short circuit of water vapor and polluted air to the global
400   stratosphere by convective transport over the Tibetan Plateau, P. Natl. Acad. Sci. USA, 103,
401   5664–5669, doi:10.1073/pnas.0601584103, 2006.
402   Fujita, E. M., Croes, B. E., Bennett, C. L., Lawson, D. R., Lurmann, F. W., and Main, H. H.:
403   Comparison of emission inventory and ambient concentration ratios of CO, NMOG, and NOx
404   in California's South Coast Air Basin. Journal of the Air & Waste Management Association,
405   42(3), 264-276, doi: 10.1080/10473289.1992.10466989, 1992.
406   Ganzeveld, L. and Lelieveld, J.: Dry deposition parameterization in a chemistry general circulation
407   model and its influence on the distribution of reactive trace gases, J. Geophys. Res., 100,
408   20999–21012, doi:10.1029/95JD02266, 1995.
409   Garny, H. and Randel, W. J.: Dynamic variability of the Asian monsoon anticyclone observed in
410   potential vorticity and correlations with tracer distributions, J. Geophys. Res. Atmos., 118,
411   13,421–13,433, doi:10.1002/2013JD020908, 2013.
414   Gettelman, A., Kinnison, D. E., Dunkerton, T. J., and Brasseur, G. P.: Impact of monsoon circulations
415   on the upper troposphere and lower stratosphere, J. Geophys. Res., 109, D22101,
416   doi:10.1029/2004jd004878, 2004.
417   Ghude, S. D., Kulkarni, S. H., Jena, C., Pfister, G. G., Beig, G., Fadnavis, S., and van der A R. J.:
418   Application of satellite observations for identifying regions of dominant sources of nitrogen
419   oxides over the Indian Subcontinent, J. Geophys. Res., 118, 1–15, doi:10.1029/2012JD017811,
420   2013.
421   Goswami, B. N., Krishnamurthy, V., and Annamalai, H.: A broad-scale circulation index for the
422   interannual variability of the Indian summer monsoon. Q. J. R. Meteorol. soc., 125, 611-633,
423   doi: 10.1002/qj.49712555412, 1999.
424   Gu, D., Wang, Y., Smeltzer, C., and Boersma, K. F.: Anthropogenic emissions of NOx over China:
425   Reconciling the difference of inverse modeling results using GOME-2 and OMI
426   measurements, J. Geophys. Res. Atmos., 119, doi:10.1002/ 2014JD021644, 2014.
427   Guo, W. W., Yuan, M., Wang, H. Y., Sun, J. H., Xie, Y. Q., Fan, W. X., and Chen, X. M.: A Study of
428   Ozone Amount in the Transition Layer Between Troposphere and Stratosphere and Its Heating
429   Rate, Chinese Journal of Geophysics, 51(5), 916-930, 2008.
432   Hilboll, A., Richter, A., and Burrows, J. P.: Long-term changes of tropospheric NO2 over megacities
433   derived from multiple satellite instruments, Atmos. Chem. Phys., 13, 4145–4169,
434   doi:10.5194/acp-13-4145-2013, 2013.
435   Horowitz, L. W., Walters, S., Mauzerall, D. L., Emmons, L. K., Rasch, P. J., Granier, C., Tie, X.,
436   Lamarque, J., Schultz, M. G.,Tyndall, G. S., Orlando, J. J., and Brasseur, G. P.: A global
437   simulation of tropospheric ozone and related tracers, Description and evaluation of MOZART,
438   version 2, J. Geophys. Res., 108, 4784, doi:10.1029/2002JD002853, 2003.
439   Jacob, D. J., Logan, J. A., and Murti, P. P.: Effect of rising Asian emissions on surface ozone in the
440   United States, Geophys. Res. Lett., 26, 2175–2178, doi:10.1029/1999GL900450, 1999.
441   Konopka, P., Grooß, J.U., Günther, G., Ploeger, F., Pommrich, R., Müller, R. and Livesey, N.: Annual
442   cycle of ozone at and above the tropical tropopause: observations versus simulations with the
443   Chemical Lagrangian Model of the Stratosphere (CLaMS), Atmos. Chem. Phys., 10(1), 121-
444   132, doi: www.atmos-chem-phys.net/10/121/2010/, 2010.

Atmospheric
Chemistry
and Physics
Discussions

445 Kunze, M., Braesicke, P., Langematz, U., Stiller, G., Bekki, S., Brühl, C., Chipperfield, M., Dameris,
446   M., Garcia, R. and Giorgetta, M.: Influences of the Indian summer monsoon on water vapor
447   and ozone concentrations in the UTLS as simulated by chemistry-climate models, J Clim,
448   23(13), 3525-3544, doi: http://dx.doi.org/10.1175/2010JCLI3280.1, 2010.
450 Lacis Andrew, A., Donald Wuebbles, J., and Jennifer Logan A., Radiative Forcing of climate by
451   Changes in the Vertical Distribution of Ozone, J. Geophys. Res., 95 , 9971-9981, doi:
452   10.1029/JD095iD07p09971, 1990.
453 Lawrence, M. G.: Atmospheric science: Asia under a high-level brown cloud, Nat. Geosci., 4, 352–
454   353, doi:10.1038/ngeo1166, 2011.
455 Lee, Y. C., Shindell, D. T., Faluvegi, G., Wenig, M., Lam, Y. F., Ning, Z., Hao, S., and Lai, C. S.:
456   Increase of Ozone concentrations, Its Temperature Sensitivity And The Precursor Factor In
457   South China, Tellus B, 66, 23455, doi: http://Dx.Doi.Org/10.3402/Tellusb.V66.23455, 2014.
458 Lei, W., Zhang, R., Tie, X., and Hess, P.: Chemical characterization of ozone formation in the
459   Houston-Galveston area. J.Geophys.Res., 109, doi: 10.1029/2003JD004219, 2004.
460 Li, C. and Yanai M.: The onset and interannual variability of the Asian summer monsoon in relation to
461   land–sea thermal contrast, J. Clim. 9: 358–375, doi: http://dx.doi.org/10.1175/1520-
462   0442(1996)009<0358:TOAIVO>2.0.CO;2, 1996.
463 Li, Q., Jiang, J. H., Wu, D. L., Read, W. G., Livesey, N. J., Waters, J. W., Zhang, Y., Wang, B.,.
464   Filipiak, M. J, Davis, C. P., Turquety, S., Wu, S., Park, R. J., Yantosca, R. M., and Jacob, D. J.:
465   Convective outflow of south Asian pollution: a global CTM simulation compared with EOS
466   MLS observations, Geophys. Res. Lett., 32, doi: http://dx.doi.org/10.1029/2005GL022762,
467   doi: 10.1029/2005GL022762, 2005.
468 Livesey, N. J., Read, W. G., Froideveaux, L., Lambert, A., Manney, G. L., Pumphrey, H. C., Santee, M.
469   L., Schwartz, M. J., Wang, S., Cofield, R. E., Cuddy, D. T., Fuller, R. A., Jarnot, R. F., Jiang, J.
470   H., Knosp, B. W., Stek, P. C., Wagner, P. A., and Wu, D. L.: Version 3.3 Level 2 data quality
471   and description document. Tech Rep. JPL D-33509, Jet Propulsion Laboratory, available at:
472   http://mls.jpl.nasa.gov (last access: 17 August 2015), 2011.
473 Livesey, N. J., Read, W. G., Filipiak, M. J., Froidevaux, L., Harwood, R. S., Jiang, J. H., Jimenez, C.,
474   Pickett, H. M., Pumphrey, H. C., Santee, M. L., Schwartz, M. J., Waters, J. W., and Wu, D. L.:
475   EOS MLS Version 1.5 Level 2 data quality and description document, JPL, California, 2005.
476 Meehl, G. A.: Coupled land-ocean-atmosphere processes and South Asian monsoon variability,
477   Science, 266, 263–267, doi: 10.1126/science.266.5183.263, 1994.
480 Park, M., Randel, W. J., Gettelman, A., Massie, S. T., and Jiang, J.H.: Transport above the Asian
481   summer monsoon anticyclone inferred from Aura Microwave Limb Sounder tracers, J.
482   Geophys.Res., 112, D16309,doi:10.1029/2006jd008294, 2007.
483 Park, M., Randel, W. J., Emmons, L. K., and Livesey, N. J.:Transport pathways of carbon monoxide in
484   the Asian summer monsoon diagnosed from Model of Ozone and Related Tracers (MOZART),
485   J. Geophys. Res., 114, D08303, doi:10.1029/2008jd010621, 2009.
486 Penki, R. K. and Kamra, A. K.: Lightning distribution with respect to the monsoon trough position
487   during the Indian summer monsoon season, J. Geophy. Res., 118, 4780–4787,
488   doi:10.1002/jgrd.50382, 2013.
489 Pozzoli, L., Bey, I., Rast, J. S., Schultz, M. G., Stier, P., and Feichter, J.: Trace gas and aerosol
490   interactions in the fully coupled model of aerosol-chemistry-climate ECHAM5- HAMMOZ: 1.
491   Model description and insights from the spring 2001 TRACE-P experiment, J. Geophys. Res.,
492   113, D07308, doi:10.1029/2007JD009007, 2008a.
493 Pozzoli, L., Bey, I., Rast, J. S., Schultz, M. G., Stier, P., and Feichter, J.: Trace gas and aerosol
494   interactions in the fully coupled model of aerosol-chemistry-climate ECHAM5- HAMMOZ: 2.
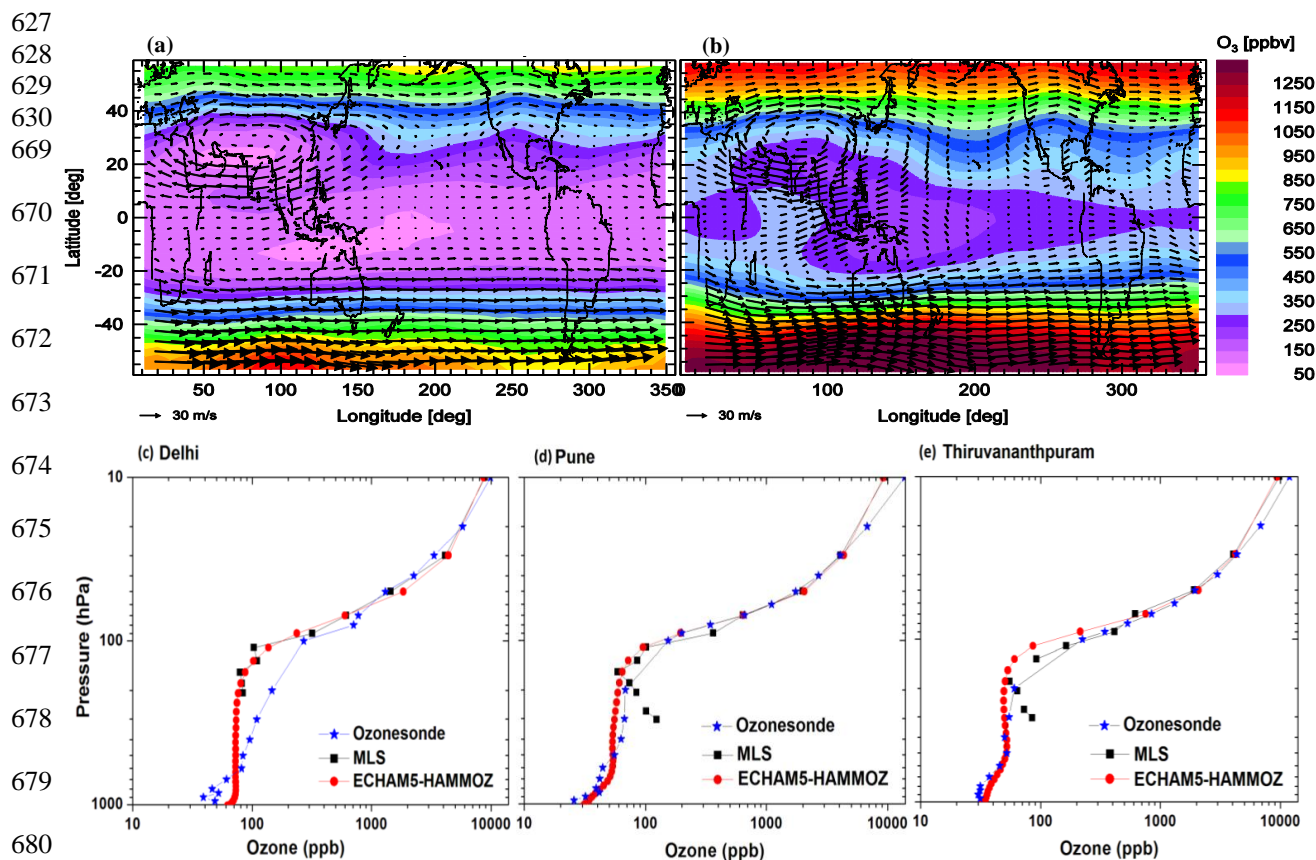495   Impact of heterogeneous chemistry on the global aerosol distributions, J. Geophys. Res., 113,

Atmospheric
Chemistry
and Physics
Discussions

Open Access

EGU

496   D07309, doi:10.1029/2007JD009008, 2008b.
497   Pozzoli, L., Janssens-Maenhout, G., Diehl, T., Bey, I., Schultz, M. G., Feichter, J., Vignati, E., and
498   Dentener, F.: Re-analysis of tropospheric sulfate aerosol and ozone for the period 1980–2005
499   using the aerosol-chemistry-climate model ECHAM5-HAMMOZ, Atmos. Chem. Phys., 11,
500   9563–9594, doi:10.5194/acp-11-9563-2011, 2011.
501   Rajagopalan, B., and Molnar, P.: Signatures of Tibetan Plateau heating on Indian summer monsoon
502   rainfall variability, J. Geophys. Res. Atmos., 118, 1170–1178, doi:10.1002/jgrd.50124, 2013.
503   Ramanathan, V., Callis, L., Cess, R., Hansen, J., Isaksen, I., Kuhn, W., Lacis, A., Luther, F., Mahlman,
504   J., Reck, R., and Schlesinger, M.: Climate-Chemical Interactions and Effects of Changing
505   Atmospheric Trace Gases, Rev. Geophys. 25, 1441–1482, doi: 10.1029/RG025i007p01441,
506   1987.
507   Ramaswamy, V. and Bowen, M.M.: Effect of changes in radiatively active species upon the lower
508   stratospheric temperatures, Journal Of Geophysical Research-All Series-, 99, 18-909, doi:
509   0418-0227/94/94JD-01310$05.00, 1994.
510   Ramaswamy, V., Boucher, O., Haigh, J., Hauglustaine, D., Haywood, J., Myhre, G., Nakajima, T., Shi,
511   G. Y., and Solomon, S.: Radiative Forcing of Climate Change, Chapter 6, in: Climate Change
512   2001, The scientific basis: Contribution of working group I to the Third assessment report of
513   the Intergovernmental Panel on Climate, edited by: Houghton, J. T., Ding, Y., Griggs, Y.,
514   Noguer, M., v.d. Linden, P. J., Dai, X., Maskell, K., and Johnson, C. A., pp. 881, Cambridge
515   University Press, Cambridge, United Kingdom and New York, NY, US, doi:
516   10.1256/004316502320517344, 2001.
517   Ranalkar, M. R. and Chaudhari, H. S.: Seasonal variation of lightning activity over the Indian
518   subcontinent, Meteorol. Atmos.Phys., 104, 125–134, doi: 10.1007/s00703-009-0026-7, 2009.
519   Randel, W. J., Wu, F., Gettelman, A., Russell, J. M., Jawodny, J. M., and Oltmans, S. J.: Seasonal
520   variation of water vapor in the lower stratosphere observed in Halogen Occultation Experiment
521   data, J. Geo-phys. Res., 106, 14,313 – 14,325, doi: 0148-0227/01/2001JD900048509.00, 2001.
522   Randel, W. J., and Park M.: Deep convective influence on the Asian summer monsoon anticyclone and
523   associated tracer variability observed with Atmospheric Infrared Sounder (AIRS), J. Geophys.
524   Res.,111, D12314, doi:10.1029/2005JD006490, 2006.
525   Randel‚ W. J., Park, M., Emmons, L., Kinnison, D., Bernath, P., Kaley Walker, A., Boone, C., and
526   Pumphrey, H.: Asian Monsoon Transport of Pollution to the Stratosphere Science, 328(5978),
527   611-613, doi: 10.1126/science.1182274, 2010.
528   Ricchiazzi, P., Yang, S., Gautier, C., and Sowle, D.: SBDART, A research and teaching tool for plane-
529   parallel radiative transfer in the Earth's atmosphere, Bull. Am. Meteorol. Soc., 79, 2101–2114.
530   1998.
531   Richter, A., John Burrows, P., Hendrik, N., Granier C., and Niemeier, U.: Increase in tropospheric
532   nitrogen dioxide over China observed from space; 437, doi:10.1038/nature04092, 2005.
533   Riese, M., Ploeger, F., Rap, A., Vogel, B., Konopka, P., Dameris, M. and Forster, P.: Impact of
534   uncertainties in atmospheric mixing on simulated UTLS composition and related radiative
535   effects, J. Geophys. Res.: Atmos., 117(D16), doi: 10.1029/2012JD017751, 2012.
536   Roeckner, E., Bauml, G., Bonaventura, L., Brokopf, R., Esch, M., Giorgetta, M., Hagemann, S.,
537   Kirchner, I., Kornblueh, L., Manzini, E., Rhodin, A., Schlese, U., Schulzweida, U., and
538   Tompkins, A.: The atmospehric general circulation model ECHAM5: Part 1, Tech. Rep. 349,
539   Max Planck Institute for Meteorology,Hamburg, 2003.
540   Roldugin, V., and Henriksen, K.: Horizontal movements in the ozone layer, accepted for publication
541   in, J. Atm. terr. Phys , 1995.
542   Sander, S. P., Fried, R. R., Barker, J. R., Golden, D. M., Kurylo, M. J.,Wine, P. H., J. Abbatt, P. D., 25
543   Burkholder, J. B., Kolb, C. E., Moortgat, G. K., Huie, R. E., and Orkin, V. L.: Chemical

Atmospheric
Chemistry
and Physics
Discussions

544   kinetics and photochemical data for use in atmospheric studies, evaluation number 14, JPL
545   Publ. 02-25, Jet Propul. Lab., Calif. Inst. Of Technol., Pasadena, available at:
546   http://jpldataeval.jpl.nasa.gov/pdf/JPL_02-25_rev02.pdf, 2003.

547 Schneider, P. and van der A. R. J.: A global single-sensor analysis of 2002–2011 tropospheric nitrogen
548   dioxide trends observed from space, J, Geophy. Res., 117, D16309,
549   doi:10.1029/2012JD017571, 2012.

550 Schoeberl, M. R., Duncan, B. N., Douglass, A. R., Waters, J., Livesey, N., Read, W., and Filipiak, M.:
551   The carbon monoxide tape recorder. Geophys. Res. Lett., 33(12), doi:
552   10.1029/2006GL026178, 2006.

553 Sillman, S.: The use of NOy, H_2O_2, and HNO_3 as indicators for ozone-NO_x-hydrocarbon sensitivity in
554   urban locations. J. Geophys. Res., 100, 14,175–14,188, doi: 10.1029/94JD02953, 1995.

555 Sinha, V., Kumar, V., and Sarkar, C.: Chemical composition of pre-monsoon air in the Indo-Gangetic
556   Plain measured using a new air quality facility and PTR-MS: high surface ozone and strong
557   influence of biomass burning, Atmos. Chem. Phys., 14, 5921–5941, 2014. doi:10.5194/acp-14-
558   5921-2014, 2014.

559 Søvde, O. A., Hoyle, C. R., Myhre, G., and Isaksen, I. S. A.: The HNO3 forming branch of the HO2 +
560   NO reaction: pre-industrial-to-present trends in atmospheric species and radiative forcings,
561   Atmos. Chem. Phys., 11, 8929–8943, 2011; doi:10.5194/acp-11-8929-2011, 2011.

562 Stevenson, D. S., P. J. Young, Vaishali, N., Lamarque, J. F., Drew, T., Shindell, Voulgarakis, A., and
563   Skeie R. B.: Tropospheric ozone changes, radiative forcing and attribution to emissions in the
564   Atmospheric Chemistry and Climate Model Intercomparison Project (ACCMIP), Atmos.
565   Chem. Phys., 13, 3063-3085, doi:10.5194/acp-13-3063-2013, 2013.

566 Stier, P., Feichter, J., Kinne, S., Kloster, S., Vignati, E., Wilson, J., Ganzeveld, L., Tegen, I., Werner,
567   M., Balkanski, Y., Schulz, M., Boucher, O., Minikin, A., and Petzold, A.: The aerosol-climate
568   model ECHAM5-HAM, Atmos. Chem. Phys., 5, 1125–1156, doi:10.5194/acp-5-1125-2005,
569   2005.

571 Thuburn, J. and Craig, G.C.: On the temperature structure of the tropical substratosphere, Journal of
572   Geophysical Research: Atmospheres, 107(D2), doi: 10.1029/2001JD000448, 2002.

573 Tie, X. X., Zhang, R., Brasseur, G., Emmons, L., and Lei, W.:Effects of lightning on reactive nitrogen
574   and nitrogen reservoir species in the troposphere, J. Geophys. Res.-Atmos., 106, 3167– 3178,
575   doi:10.1029/2000JD900565, 2001.

576 Tie, X., Madronich, S., Li, G.H., Ying, Z.M., Zhang, R., Garcia, A., Lee-Taylor, and J., Y. Liu.
577   Characterizations of chemical oxidants in Mexico City: a regional chemical/dynamical model
578   (WRF-Chem) study, Atmos. Environ., 41, 1989–2008, doi:10.1016/j.atmosenv.2006.10.053,
579   2007.

580 Tobo, Y., Iwasaka, Y., Zhang, D., Shi, G., Kim, Y. S., Tamura, K., and Ohashi, T.: Summertime
581   ''ozone valley'' over the Tibetan Plateau derived from ozonesondes and EP/TOMS data,
582   Geophys. Res. Lett., 35, L16801, doi:10.1029/2008GL03434, 2008.

583 Vernier, J.-P., T. D. Fairlie, M. Natarajan, F. G. Wienhold, J. Bian, B. G. Martinsson, S. Crumeyrolle,
584   L. W. Thomason, and Bedka, K.: Increase in upper tropospheric and lower stratospheric
585   aerosol levels and its potential connection with Asian Pollution, J. Geophys. Res. Atmos., 120,
586   1608–1619, doi:10.1002/2014JD022372, 2015.

587 Vinoj, V., Rasch, P.J., Wang, H., Yoon, J.H., Ma, P.L., Landu, K. and Singh, B.: Short-term modulation
588   of Indian summer monsoon rainfall by West Asian dust, Nature Geoscience, 7(4), 308-313,
589   doi:10.1038/ngeo2107, 2014.

590 Vogel B., Günther G., Müller R., Grooß, and Riese M.: Impact of different Asian source regions on the
591   composition of the Asian J.-U. monsoon anticyclone and of the extratropical lowermost
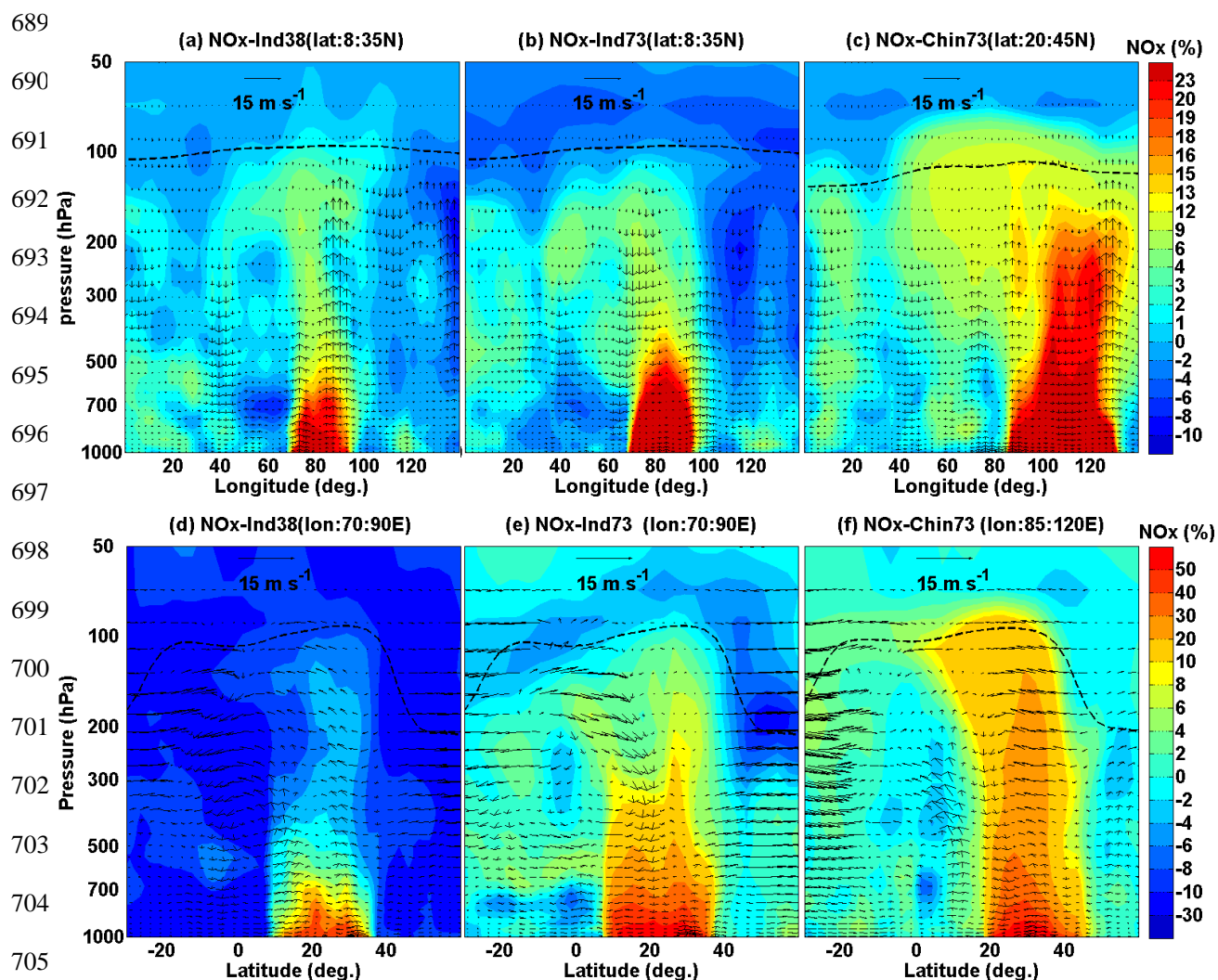592   stratosphere, Atmos. Chem. Phys., 15, 13699–13716, doi:10.5194/acp-15-13699-2015, 2015.

Atmospheric
Chemistry
and Physics
Discussions

Open Access

EGU

593 Wang, Y. X., McElroy, M. B., Martin, R.V., Streets, D. G., Zhang, Q., and Fu, T. M.: Seasonal
594   variability of NOx emissions over east China constrained by satellite observations:
595   Implications for combustion and microbial sources, J. Geophys. Res., 112, D06301,
596   doi:10.1029/2006jd007538, 2007.
597 Waters, J. W., Froidevaux, L., Harwood, R.S., Jarnot, R.F., Pickett, H. M., Read, W. G., Siegel, P. H.,
598   Cofield, R. E., Filipiak, M. J., Flower, D. A., Holden, J. R., Lau, G. K., Livesey, N. J., Manney,
599   G. L., Pumphrey, H. C., Santee, M. L., Wu, D. L., Cuddy, D. T., Lay, R. R., Loo, M. S., Perun,
600   V. S., Schwartz, M. J., Stek, P. C., Thurstans, R. P., Boyles, M. A., Chandra, S., Chavez, M. C.,
601   Chen, G. S., Chudasama, B. V., Dodge, R., Fuller, R. A., Girard, M.A., Jiang, J. H., Jiang, Y.,
602   Knosp, B. W., LaBelle, R. C., Lee, K. A., Miller, D., Oswald, J. E., Patel, N. C., Pukala, D.
603   M., Quintero, O., Scaff, D. M., Snyder, W. V., Tope, M. C., Wagner, P. A., and Walch, M. J.:
604   The Earth Observing System Microwave LimbSounder (EOS MLS) on the Aura satellite.IEEE
605   Trans, Geosci.Remote Sensing44, 1075 – 1092, doi: 10.1109/TGRS.2006.873771, 2006.
606 Wild, O., and Akimoto, H.: Intercontinental transport of ozone and its precursors in a three-
607   dimensional global CTM, Jour. Geophys. Res.: Atmos., 106(D21), 27729-27744, doi:
608   http://dx.doi.org/10.1029/2000JD000123, 2001.
609 Wu, G. X., and Zhang, Y. S.: Tibetan Plateau forcing and the timing of the monsoon onset over South
610   Asia   and   the   South   ChinaSea,   Mon   Wea   Rev   126:913–927,   doi:
611   http://dx.doi.org/10.1175/1520-0493(1998)126<0913:TPFATT>2.0.CO;2, 1998.
612 Yamaji, K., Ohara, T., Uno, I., Tanimoto, H., Kurokawa, J., and Akimoto, H.: Analysis of the seasonal
613   variation of ozone in the boundary layer in East Asia using the Community Multiscale Air
614   Quality model: what controls surface ozone levels over Japan?, Atmos. Environ., 40, 1856–
615   1868, 2006.
616 Yanai, M., Li, C., Song, Z.: Seasonal heating of the Tibetan Plateau and its effects on the evolution of
617   the Asian summer monsoon, J Meteor Soc Japan, 70, 189–221, 1992.
618 Zhang, R.W., Lei, X., and TieHess, P.: Industrial emissions cause extreme diurnal urban ozone
619   variability. Proc. Natl. Acad. Sci. USA, 101, 6346–6350, doi: 10.1073/pnas.0401484101, 2004.
620 Zhao, C. and Wang, Y. H.: Assimilated inversion of NOx emissions over East Asia using OMI NO2
621   column measurements, Geophys.Res. Lett., 36, L06805, doi:10.1029/2008gl037123, 2009.
622 Zhao, B., Wang, S. X., Liu, H., Xu, J. Y., Fu, K., Klimont, Z., Hao, J. M., He, K. B., Cofala, J., and
623   Amann, M.: NOx emissions in China: historical trends and future perspectives, Atmos. Chem.
624   Phys., 13, 9869–9897, doi:10.5194/acp-13-9869-2013, 2013.
625
626

Atmospheric
Chemistry
and Physics
Discussions

627
628
629
630
669
670
671
672
673

674
675
676
677
678
679
680

681   Figure 1: Distribution of ozone mixing ratio (ppbv) during the monsoon season (June-September)

682   obtained from (a) MLS observations at 100 hPa. Black arrows indicate wind vectors from ERA-

683   Interim. Show the same but obtained from (b) ECHAM5-HAMMOZ CTRL simulation at 90 hPa.

684   Black arrows indicate simulated wind vectors. ECHAM5-HAMMOZ simulation is smoothed with

685   averaging kernel of MLS. Vertical distribution of seasonal mean (June-September) ozone mixing ratios

686   (ppb) as obtained from ozonesonde (2001-2009), MLS (2004-2013) and ECHAM5-HAMMOZ CTRL

687   simulation at Indian stations, (c) Delhi (d) Pune (e) Thiruvananthpuram.

688

Atmospheric
Chemistry
and Physics
Discussions

689

690

691

692

693

694

695

696

697

698

699

700

701

702

703

704

705

Figure 2: Longitude pressure cross-section of NO_x anomalies (%) averaged for the monsoon season (June-September) obtained from (a) Ind38 (averaged over 8°N-35°N), (b) Ind73 (averaged over 8°N-35°N), (c) Chin73 (averaged over 20°N-45°N) simulations. Latitude pressure cross-section of NO_x anomalies (%) averaged for the monsoon season (June-September) obtained from (d) Ind38 (averaged over 70°E-90°E), (e) Ind73 (averaged over 70°E-90°E), (f) Chin73 (averaged over 85°E-120°E) simulations. Black arrows indicate wind vectors. The vertical velocity field has been scaled by 300. The dashed line represents the tropopause.

713

714

715

716

717

718

719

720

721

722

723

724
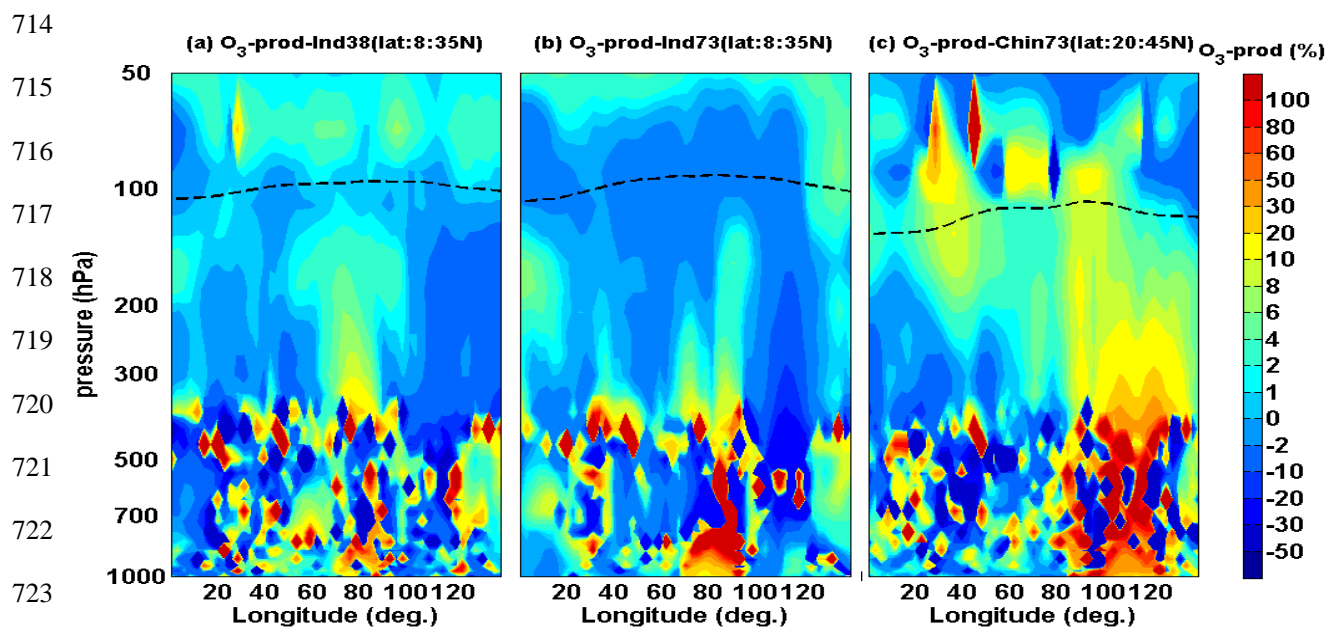
Figure 3: Longitude pressure cross-section of changes in net ozone production (%) (due to enhanced

NO$_x$ with respect to CTRL simulation) averaged for the monsoon season (June-September) obtained

from (a) Ind38 (averaged over 8ºN-35ºN), (b) Ind73 (averaged over 8ºN-35ºN), (c) Chin73 (over 20ºN-

45ºN) simulations. The dashed line represents the tropopause.

729

730
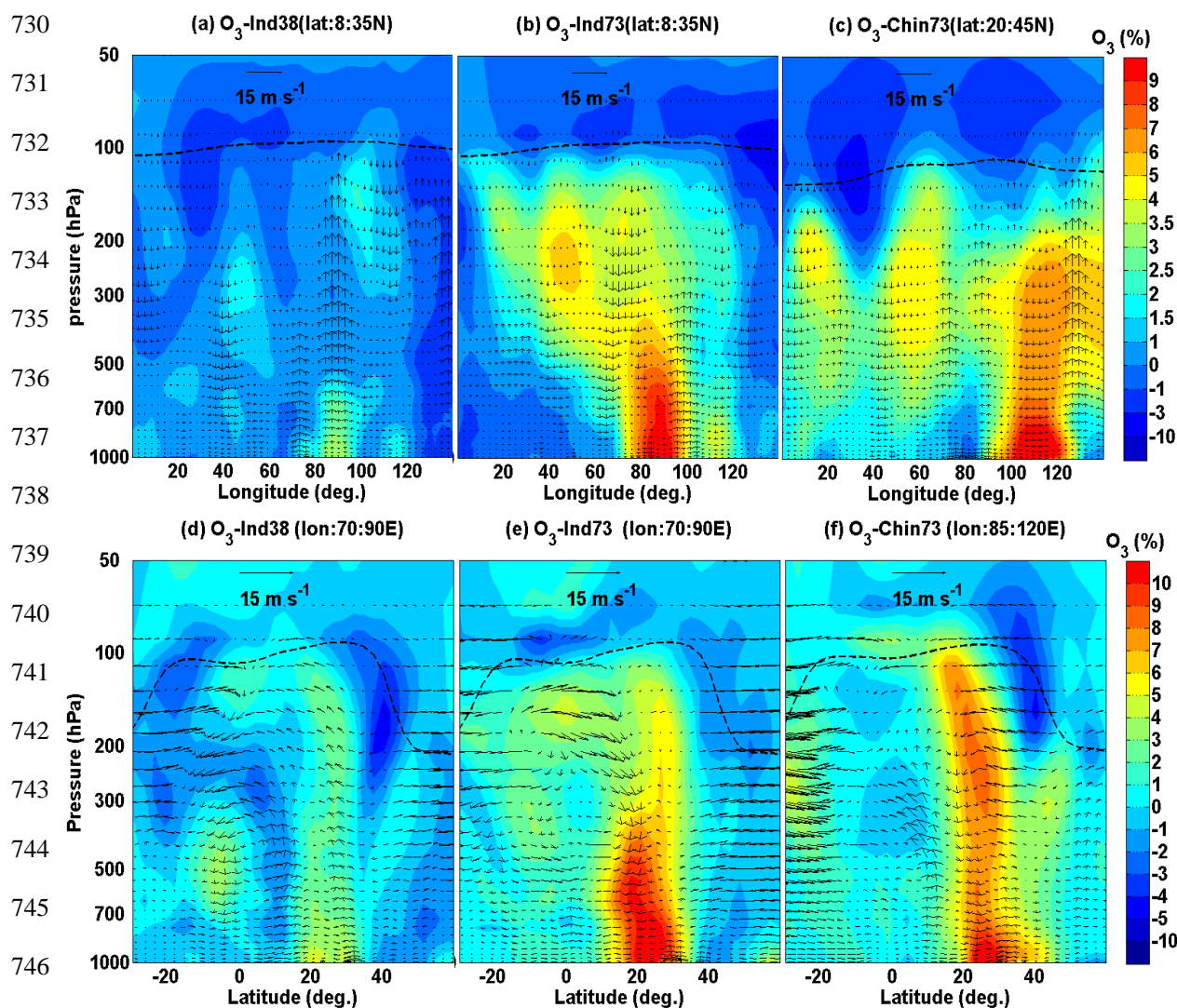
Figure 4: Longitude pressure cross-section of ozone anomalies (%) averaged for the monsoon season (June-September) obtained from (a) Ind38 (averaged over 8ºN-35ºN), (b) Ind73 (averaged over 8ºN-35ºN), (c) Chin73 (averaged over 20ºN-45ºN) simulations. Latitude pressure cross-section of ozone anomalies (%) averaged for the monsoon season (June-September) obtained from (d) Ind38 (averaged over 70ºE-90ºE), (e) Ind73 (averaged over 70ºE-90ºE), (f) Chin73 (averaged over 85ºE-120ºE) simulations. Black arrows indicate wind vectors. The vertical velocity field has been scaled by 300. The dashed line represents the tropopause.

754

755

756

757
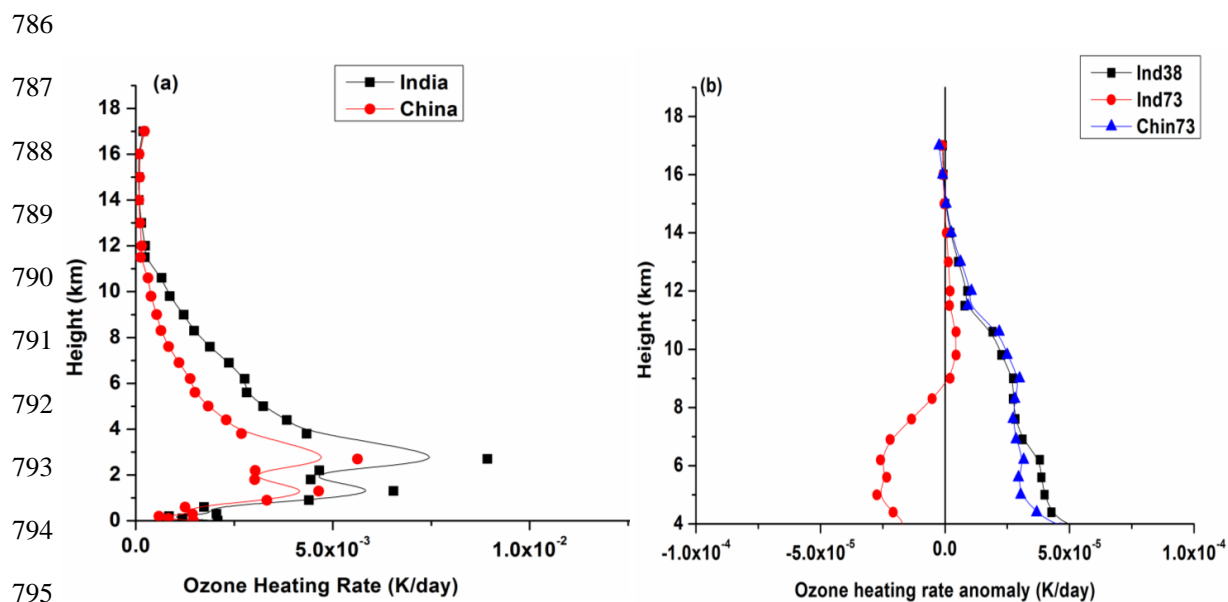
758

759

760

761

762

763

764

765
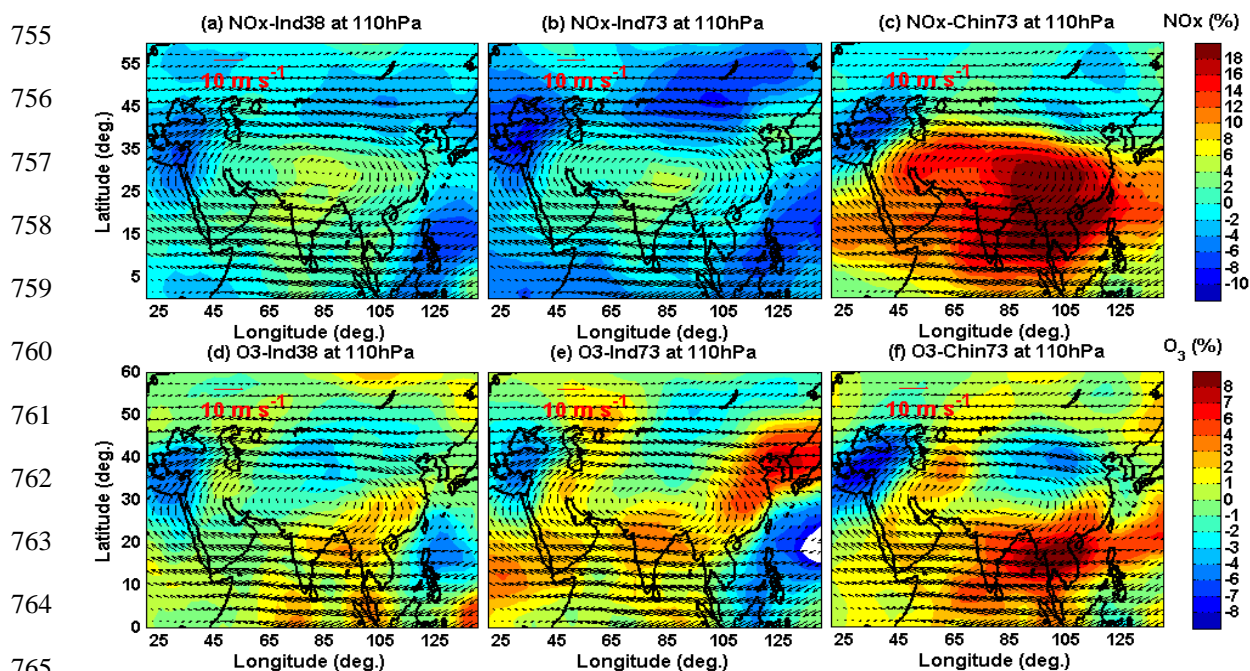
766   Figure 5: Latitude-longitude cross-section of NO$_x$ anomalies (%) averaged for the monsoon season

767   (June-September) at 110 hPa obtained from (a) Ind38 (b) Ind73 (c) Chin73 simulations. (d-f) Show the

768   same but for ozone (%) at 110 hPa for (d) Ind38 (e) Ind73 (f) Chin73 simulations. Black arrows

769   indicate horizontal winds at 110 hPa.

770

771

780
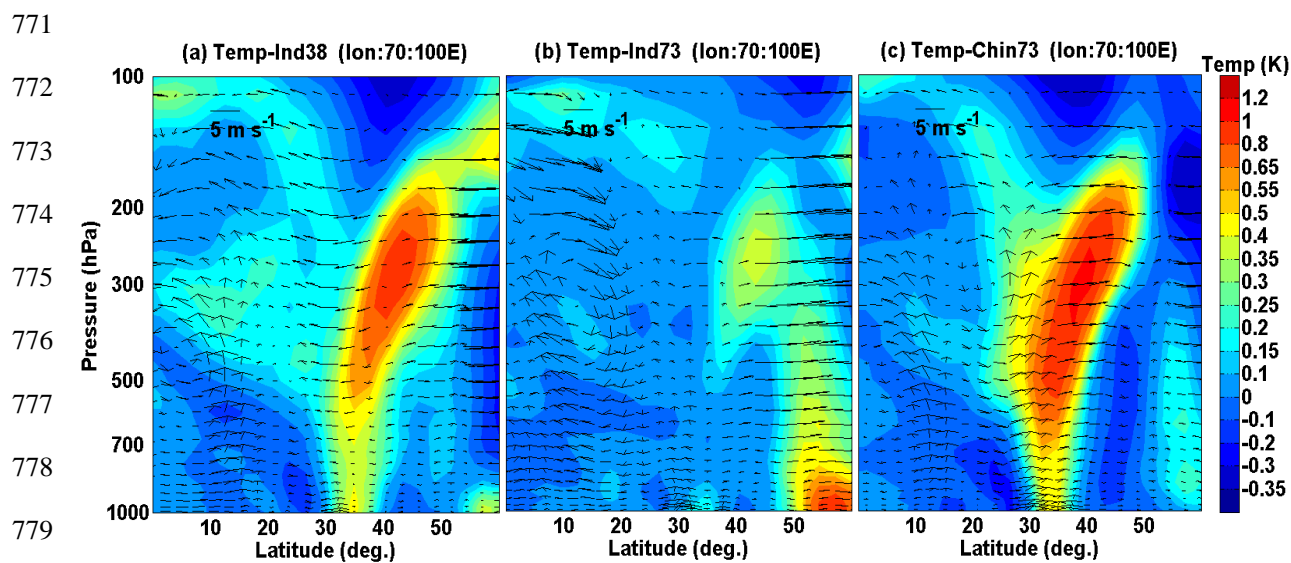
Figure 6: Latitude pressure cross-section of temperature anomalies (K) averaged for the monsoon season (June-September) obtained from (a) Ind38 (averaged over 70ºE-94ºE) (b) Ind73 (averaged over 70ºE-94ºE) and (c) Chin73 (averaged over 70ºE-100ºE) simulations. Black arrows indicate wind vectors. The vertical velocity field has been scaled by 300.

785

Atmospheric
Chemistry
and Physics
Discussions

786

787

788

789

790

791

792

793

794

795

796   Figure 7: Vertical profile of (a) ozone heating rate (K/day) obtained from CTRL simulations averaged

797   over India (70º-94ºE, 20º-30ºN) and China (70º-100ºE, 30º-40ºN), (b) ozone heating rate

798   anomaly(K/day) averaged over Tibetan Plateau (70º-100ºE, 20º-30ºN) obtained from Ind38, Ind73 and

799   Chin73 simulations.

800

Atmospheric
Chemistry
and Physics
Discussions
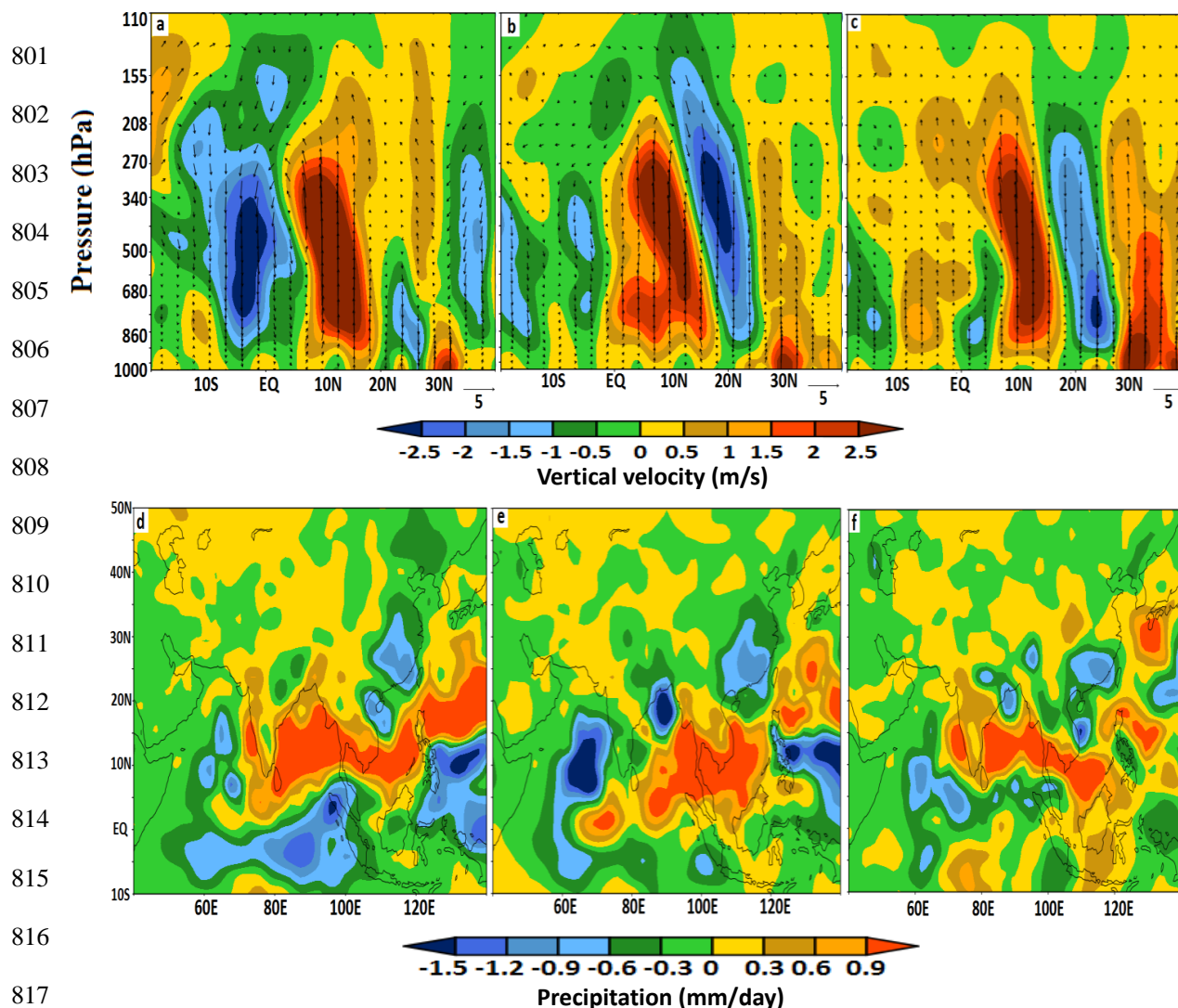
Figure 8: Change in the meridional circulation due to enhanced NO_X emissions averaged for the monsoon season (June-September) and over 70ºE-110ºE for (a) Ind38 (b) Ind73 (c) Chin73 simulations. Shaded contours indicate the anomalies in vertical velocity (m/s). The vertical velocity field has been scaled by 300. Precipitation anomalies (mm/day) averaged for the monsoon season (June-September) obtained from (d) India38 (e) Ind73 (f) Chin73 simulations with respect to CTRL.